Science Advances

AAAS

advances.sciencemag.org/cgi/content/full/4/2/eaao3225/DC1

Supplementary Materials for

Systematic deficiency of aftershocks in areas of high coseismic slip for large subduction zone earthquakes

Nadav Wetzler, Thorne Lay, Emily E. Brodsky, Hiroo Kanamori

Published 14 February 2018, *Sci. Adv.* **4**, eaao3225 (2018)
DOI: 10.1126/sciadv.aao3225

The PDF file includes:

Other Supplementary Material for this manuscript includes the following:
(available at advances.sciencemag.org/cgi/content/full/4/2/eaao3225/DC1)

table S1. Mainshock information. Event ID number corresponds with event number listed in Fig. S1 (mainshock bundle). The preferred rupture velocity ("Vr") in km/sec is shown corresponding with the right column ("Ref.") indicating the reference number for the mainshock coseismic slip model. The normalized source dimension "R_j" is the radius (km) of a circle with equivalent area to that of the χ=0.15, and the values plotted in Fig. 8.

ID	Date	Location	Mw	Lat.	Long.	Vr	Ref.	R_j	$\sum_{IN} M_0^{inter} / M_0^*$	$\sum_{IN} M_0^{inter} / \sum_{ALL} M_0^{inter}$
1	5-Mar-90	Vanuatu	7.0	-18.32	168.16	2.5	16	12.6	0.00E+00	0.00E+00
2	25-Mar-90	Costa Rica	7.3	9.94	275.22	2.5	16	29.7	0.00E+00	0.00E+00
3	18-Apr-90	Sulawesi	7.7	1.20	122.82	2.5	16	41.1	1.98E-02	9.80E-01
4	20-Jun-91	Sulawesi	7.5	1.21	122.77	2.5	16	17.6	0.00E+00	0.00E+00
5	19-Nov-91	Colombia	7.2	4.55	282.64	2.5	16	20.1	0.00E+00	0.00E+00
6	22-Dec-91	Kuril	7.6	45.59	151.04	2.5	16	47.3	0.00E+00	0.00E+00
7	25-Apr-92	California	7.2	40.35	235.93	2.5	16	15.6	0.00E+00	0.00E+00
8	15-May-92	Guinea	7.2	-6.06	147.62	2.5	16	20.5	0.00E+00	0.00E+00
9	17-May-92	Mindanao	7.1	7.33	126.67	2.5	16	15.8	0.00E+00	0.00E+00
10	2-Sep-92	Nicaragua	7.7	11.74	272.66	1.6	16	66.6	4.22E-03	6.96E-01
11	12-Dec-92	Indonesia	7.8	-8.50	121.83	2.5	16	33.7	0.00E+00	0.00E+00
12	11-May-93	Mindanao	7.0	7.25	126.62	2.5	16	18.7	1.55E-02	1.00E+00
13	10-Aug-93	New Zealand	7.0	-45.22	167.01	2.5	16	18.9	9.27E-03	1.00E+00
14	10-Sep-93	Mexico	7.3	14.76	267.36	2.5	16	16.0	0.00E+00	0.00E+00
15	13-Nov-93	Kamchatka	7.0	51.94	158.63	2.5	16	18.5	0.00E+00	0.00E+00
16	2-Jun-94	Java	7.8	-10.41	112.94	2.0	16	65.6	0.00E+00	0.00E+00
17	28-Dec-94	Honshu	7.8	40.54	143.43	2.5	16	39.2	1.10E-02	6.67E-01
18	5-May-95	Samar	7.1	12.66	125.22	2.5	16	25.2	3.44E-03	6.23E-01
19	3-Jul-95	Kermadec	7.2	-29.40	182.55	2.5	16	19.2	0.00E+00	0.00E+00
20	30-Jul-95	Chile	8.0	-23.34	289.73	2.5	16	65.1	1.91E-03	2.67E-01
21	16-Aug-95	Solomon	7.7	-5.78	154.29	2.5	16	43.9	2.72E-02	8.59E-01
22	9-Oct-95	Mexico	8.0	19.05	255.79	2.5	16	62.9	0.00E+00	0.00E+00
23	3-Dec-95	Kuril	7.9	44.71	149.26	2.5	16	57.0	1.25E-03	1.32E-01
24	1-Jan-96	Sulawesi	7.8	0.71	119.90	2.5	16	21.6	0.00E+00	0.00E+00
25	7-Feb-96	Kuril	7.2	45.37	149.90	2.5	16	20.4	1.60E-03	1.78E-01
26	17-Feb-96	Indonesia	8.2	-0.92	136.98	2.5	16	76.5	0.00E+00	0.00E+00
27	21-Feb-96	Peru	7.5	-9.59	280.41	1.5	16	52.3	0.00E+00	0.00E+00
28	25-Feb-96	Mexico	7.1	15.93	261.89	2.5	16	18.7	0.00E+00	0.00E+00
29	29-Apr-96	Papua	7.2	-6.54	155.10	2.5	16	16.1	9.42E-04	8.48E-03
30	10-Jun-96	Aleutian	7.9	51.59	182.41	2.5	16	63.7	1.07E-01	9.83E-01
31	11-Jun-96	Samar	7.1	12.68	125.12	2.5	16	26.9	0.00E+00	0.00E+00
32	12-Nov-96	Peru	7.7	-14.96	284.44	2.5	16	46.3	2.05E-03	2.30E-01
33	20-Sep-97	Kermadec	7.0	-28.80	182.56	2.5	16	13.0	0.00E+00	0.00E+00
34	25-Nov-97	Sulawesi	7.0	1.20	122.49	2.5	16	18.3	0.00E+00	0.00E+00
35	5-Dec-97	Kamchatka	7.8	54.80	162.00	2.5	16	50.1	6.59E-03	2.80E-01
36	30-Jan-98	Chile	7.1	-23.85	289.85	2.5	16	23.7	0.00E+00	0.00E+00
37	1-Apr-98	Indonesia	7.0	-0.56	99.20	2.5	16	25.9	0.00E+00	0.00E+00
38	17-Jul-98	Papua	7.0	-2.98	142.69	2.5	16	31.3	0.00E+00	0.00E+00
39	4-Aug-98	Ecuador	7.2	-0.60	279.69	2.5	16	17.8	0.00E+00	0.00E+00
40	16-May-99	Papua	7.1	-4.71	152.61	2.5	16	32.4	0.00E+00	0.00E+00

41	19-Nov-99	Papua	7.0	-6.36	148.81	2.5	16	14.4	0.00E+00	0.00E+00
42	23-Jun-01	Peru	8.4	-16.38	286.50	2.4	20	97.4	6.86E-02	9.57E-01
43	5-Mar-02	Mindanao	7.5	6.02	124.21	2.5	16	19.8	0.00E+00	0.00E+00
44	8-Sep-02	Papua	7.6	-3.26	142.98	2.5	16	33.3	0.00E+00	0.00E+00
45	22-Jan-03	Mexico	7.5	18.90	255.94	2.5	16	25.3	0.00E+00	0.00E+00
46	17-Mar-03	Alaska	7.1	51.28	177.93	2.5	16	15.4	4.58E-02	9.25E-01
47	21-Aug-03	New Zealand	7.2	-45.20	167.14	2.5	16	19.0	0.00E+00	0.00E+00
48	25-Sep-03	Hokkaido	8.2	41.86	143.87	2.5	29	54.7	5.83E-02	8.53E-01
49	31-Oct-03	Houshu	7.0	37.87	142.59	2.5	16	24.6	0.00E+00	0.00E+00
50	17-Nov-03	Aleutian	7.8	51.12	178.65	2.5	16	45.5	9.15E-04	7.60E-01
51	27-Dec-03	Loyalty	7.3	-21.97	169.86	2.5	16	38.1	3.81E-02	2.01E-01
52	11-Nov-04	Indonesia	7.6	-8.18	124.71	2.5	16	52.9	2.96E-04	3.46E-01
53	28-Nov-04	Hokkaido	7.0	43.02	145.15	2.5	16	13.3	0.00E+00	0.00E+00
54	26-Dec-04	Sumatra	9.2	3.30	96.00	2.2	30	211.6	1.13E-03	9.48E-01
55	28-Mar-05	Sumatra	8.7	2.05	97.06	2.3	31	85.8	1.12E-04	1.45E-01
56	16-Aug-05	Honshu	7.2	38.27	142.03	2.5	16	17.4	0.00E+00	0.00E+00
57	17-Jul-06	Java	7.7	-9.32	107.33	1.2	16	52.2	4.08E-03	6.94E-01
58	15-Nov-06	Kuril	8.3	46.58	153.27	1.8	16	76.8	2.87E-04	8.84E-01
59	25-Mar-07	Vanuatu	7.2	-20.62	169.41	2.5	16	20.5	4.41E-01	7.52E-01
60	1-Apr-07	Solomon	8.1	-8.43	157.06	2.5	35	54.3	3.32E-03	8.36E-01
61	15-Aug-07	Peru	8.0	-13.38	283.39	1.0	20	53.7	1.27E-03	1.81E-01
62	2-Sep-07	Santa Cruz Is.	7.3	-11.62	165.84	2.0	16	12.9	3.68E-02	9.36E-01
63	12-Sep-07	Sumatra	8.5	-4.44	101.37	2.4	32	76.3	6.69E-04	5.64E-01
64	12-Sep-07	Sumatra	7.9	-2.66	100.83	2.5	32	45.1	0.00E+00	0.00E+00
65	13-Sep-07	Mentawai	7.1	-2.15	99.61	2.5	16	17.4	0.00E+00	0.00E+00
66	14-Nov-07	Chile	7.8	-22.25	290.11	2.5	16	39.8	4.82E-04	7.97E-03
67	19-Dec-07	Aleutian	7.2	51.36	180.49	2.5	16	17.9	3.97E-03	8.53E-02
68	20-Feb-08	Simeulue	7.3	2.77	95.96	2.5	16	34.6	0.00E+00	0.00E+00
69	25-Feb-08	Mentawai	7.2	-2.49	99.97	2.5	16	21.6	1.31E-01	3.77E-01
70	9-Apr-08	Loyalty	7.3	-20.07	168.89	2.5	16	23.5	0.00E+00	0.00E+00
71	19-Jul-08	Honshu	7.0	37.55	142.21	2.5	16	14.5	0.00E+00	0.00E+00
72	29-Sep-08	Kermadec	7.1	-29.76	182.32	2.5	16	22.2	0.00E+00	0.00E+00
73	16-Nov-08	Sulawesi	7.4	1.27	122.09	2.5	16	23.5	0.00E+00	0.00E+00
74	3-Jan-09	Papua	7.7	-0.41	132.89	2.5	16	54.3	7.07E-04	1.95E-03
75	15-Jul-09	New Zealand	7.8	-45.76	166.56	2.5	16	38.0	1.54E-04	9.97E-02
76	7-Oct-09	Vanuatu	7.6	-13.01	166.51	2.5	16	36.6	5.10E-01	1.91E-01
77	27-Feb-10	Chile	8.8	-36.12	287.10	2.5	33	113.9	7.84E-04	8.34E-01
78	6-Apr-10	N. Sumatra	7.9	2.38	97.05	2.5	16	37.5	0.00E+00	0.00E+00
79	9-May-10	N. Sumatra	7.3	3.75	96.02	2.5	16	30.7	1.86E-03	1.00E+00
80	10-Aug-10	Vanuatu	7.3	-17.54	168.07	2.5	16	13.3	0.00E+00	0.00E+00
81	25-Oct-10	Mentawai	7.9	-3.49	100.08	1.5	34	31.8	0.00E+00	0.00E+00
82	2-Jan-11	Chile	7.2	-38.36	286.67	2.5	16	16.1	0.00E+00	0.00E+00
83	11-Mar-11	Tohoku	9.1	38.30	142.37	1.5-2.5	16	116.9	8.58E-05	5.26E-03
84	20-Aug-11	Vanuatu	7.2	-18.37	168.14	2.5	16	27.0	8.76E-01	9.61E-01
85	20-Aug-11	Vanuatu	7.1	-18.31	168.22	2.5	16	22.2	1.19E+00	9.63E-01
86	20-Mar-12	Mexico	7.5	16.66	261.81	2.5	16	13.8	0.00E+00	0.00E+00

87	25-Mar-12	Chile	7.2	-35.18	288.21	2.5	16	27.8	0.00E+00	0.00E+00
88	27-Aug-12	El Salvador	7.4	12.28	271.47	2.5	16	40.5	5.85E-04	1.00E+00
89	5-Sep-12	Costa Rica	7.7	10.12	274.65	2.5	16	40.1	8.72E-04	7.89E-01
90	28-Oct-12	Haida Gwaii	7.8	52.79	227.90	2.3	16	45.1	0.00E+00	0.00E+00
91	7-Nov-12	Guatemala	7.4	14.08	268.08	2.5	16	19.9	1.65E-03	3.90E-02
92	6-Feb-13	Santa Cruz Is.	8.0	-10.74	165.14	1.5	16	40.9	0.00E+00	0.00E+00
93	30-Aug-13	Alaska	7.0	51.55	184.77	2.5	16	23.3	4.71E-02	1.45E-01
94	25-Sep-13	Peru	7.1	-15.84	285.49	2.5	16	16.6	0.00E+00	0.00E+00
95	1-Apr-14	N. Chile	8.1	-19.64	289.18	1.5	16	55.5	2.36E-02	7.24E-02
96	18-Apr-14	Guerrero	7.3	17.55	259.18	2.5	16	22.0	0.00E+00	0.00E+00
97	19-Apr-14	Papua	7.5	-6.72	154.93	2.5	16	15.0	0.00E+00	0.00E+00
98	29-Mar-15	Papua	7.5	-4.76	152.56	2.5	16	39.0	1.73E-03	2.05E-01
99	5-May-15	Papua	7.5	-5.47	151.89	2.5	16	58.3	3.69E-03	4.75E-01
100	16-Sep-15	Illapel	8.3	-31.57	288.33	1.5-3.0	16	71.7	6.87E-03	2.21E-01
101	16-Apr-16	Ecuador	7.8	0.31	279.88	2.5	16	49.8	5.33E-03	5.07E-01

fig. S1. Bundle of event sequences for 101 mainshocks. Each page has up to four panels for different events. **Upper left corner**: map showing all GCMT seismicity in each mainshock's vicinity including the 14-days aftershocks, plotted at the relocated epicenters using the GCMT focal mechanism. The plots include all aftershocks in the GCMT catalog with $M_W \geq 5.2$. The mainshock epicentral location is from the NEIC and is indicated by the black focal mechanism. The region(s) within the $\chi = 0.15$ contour of the preferred slip model is(are) plotted by the light pink polygon(s). The area in which aftershocks are considered is indicated by the magenta circle. Interplate aftershocks have red compressional quadrants, intraplate events are outlined by red. **Upper right corner**: projected locations of the aftershock hypocenters on the extended mainshock fault plane with respect to the preferred slip map (colored contours). Interplate aftershocks have solid red dots, and intraplate events have red outlines. The $\chi = 0.15$ contour of the slip model is the magenta line. See table S1 for information about the individual references for the mainshock coseismic slip model. Models from (*16*) with Vr = 2.5 km/s are our preferred models for those events. **Lower left corner**: lower hemisphere stereographic plots of the distribution of the compressional (P), tensional (T), and null (B) principal stress axes of the aftershocks with respect to the P, T, and B axes of the mainshock (solid diamonds). Events having focal mechanism solutions with P, T, and B axes all within 30° of the mainshock values are indicated by filled color symbols, and these are identified as interplate events. **Lower right corner**: histograms of numbers of aftershocks at varying minimum distances from the $\chi = 0.15$ contour normalized by the radius of a circle having equivalent area to that bounded by the contour, R_j. Interplate events are plotted along the positive Y-axis and intraplate events are plotted along the negative Y-axis. The dashed vertical line marks the position of the reference contour. The scaling radius is indicated on the X-axis.

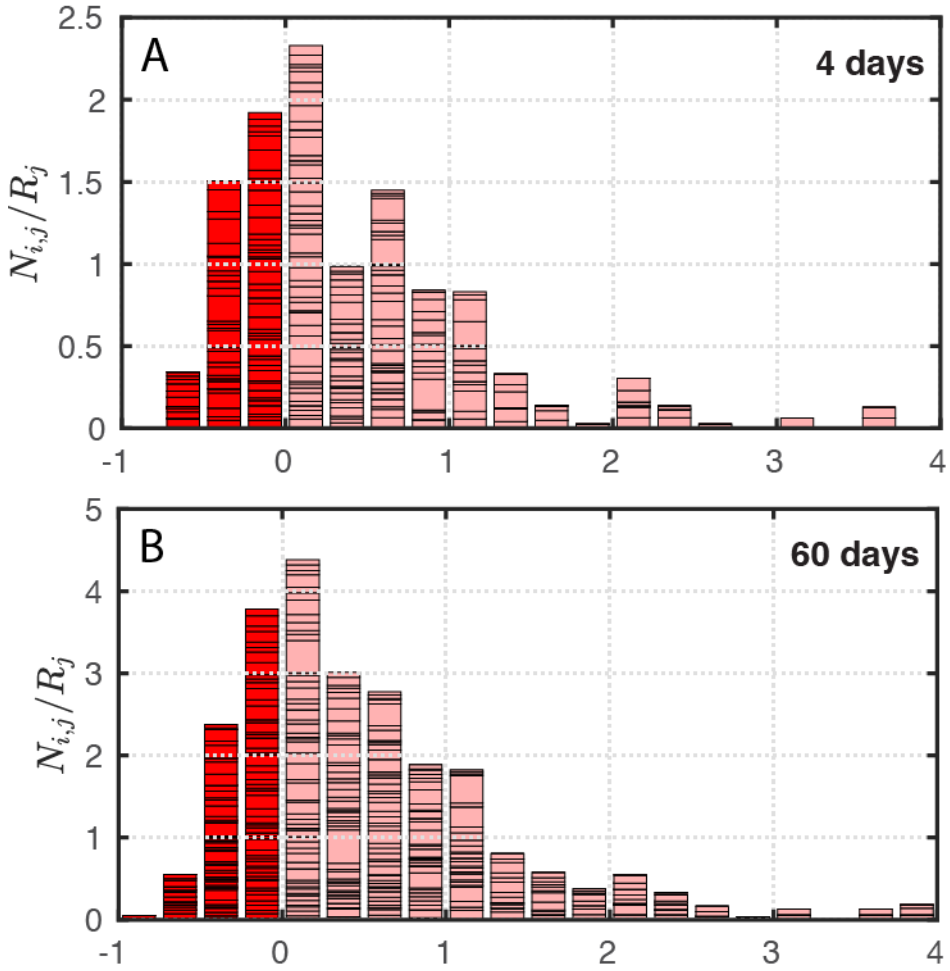

fig. S2. Seismicity locations relative to mainshock slip zones for different time windows. Distributions of minimum distance of aftershocks from the fraction of peak slip χ = 0.15 contour for 101 mainshocks calculated for two alternative time windows (**A**): 4 days, and (**B**): 60 days. The plots include all aftershocks in the GCMT catalog with $M_W \geq 5.2$. Hypocenters are projected to the extended mainshock fault plane and in-plane minimum distances from the slip contour (Δr_i) are measured, with negative values being within the enclosed contour and positive values being external to it. To compare events with different source dimensions, distances from the slip contour for a given event are normalized by R_j, the radius of a circle with equivalent area to that enclosed by the slip contour. The event counts in each category for a given event are also divided by R_j, with the horizontal lines separating the counts contributed to each histogram bar by different events. Darker red for negative values of Δr_i correspond to aftershocks located within the slip contour (essentially overlapping the mainshock slip region), and lighter red indicates aftershocks outside the contour.

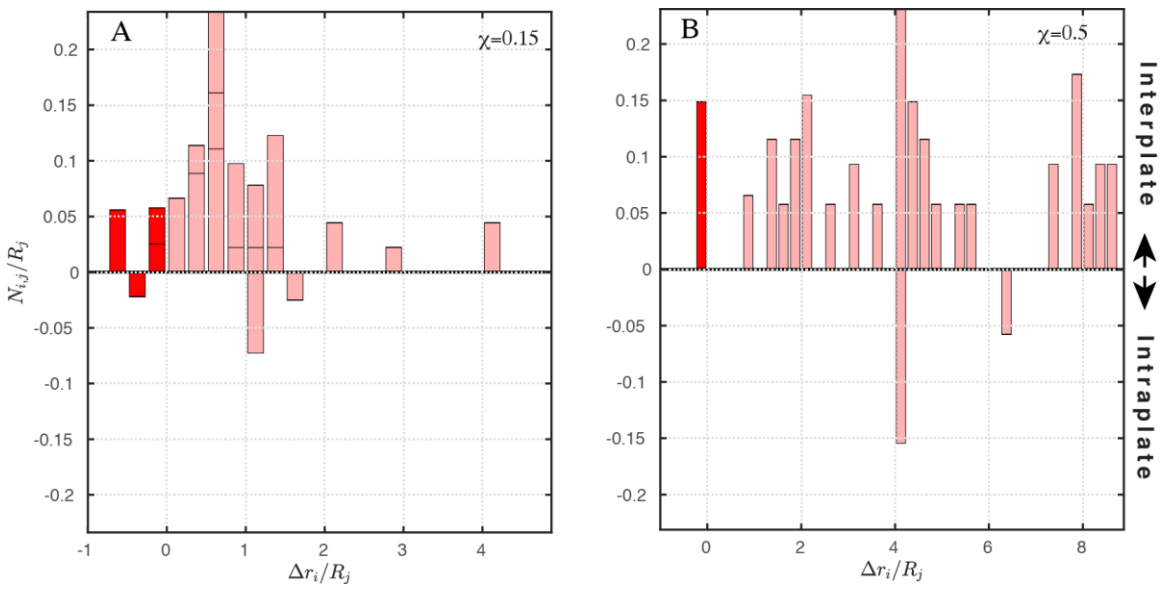

fig. S3. Seismicity locations relative to mainshock slip zones. Distributions of minimum distance of aftershocks from the fraction of peak slip: (**A**): χ = 0.15, and (**B**): χ = 0.5 contour for events that rupture Domain C. The plots include all 14-day aftershocks in the GCMT catalog with $M_W \geq 5.2$. Hypocenters are projected to the extended mainshock fault plane and in-plane minimum distances from the slip contour (Δr_i) are measured, with negative values being within the enclosed contour and positive values being external to it. To compare events with different source dimensions, distances from the slip contour for a given event are normalized by R_j, the radius of a circle with equivalent area to that enclosed by the slip contour. The event counts in each category for a given event are also divided by R_j, with the horizontal lines separating the counts contributed to each histogram bar by different events. Darker red for negative values of Δr_i correspond to aftershocks located within the slip contour (essentially overlapping the mainshock slip region), and lighter red indicates aftershocks outside the contour. The upper portion of each panel indicates interplate (thrust-faulting) seismicity, and the lower portion indicates intraplate seismicity.

fig. S4. Bundle of 25 event-specific slip deficiency estimates. For each mainshock with at least 7 interplate aftershocks, we compute the areal distribution of positions at different distances from specified rupture contours within the search areas for the aftershocks used for each event (fig. S1). Here the results for $\chi = 0.15$ contours are shown for 25 events with sufficient number of aftershocks. The randomly assigned positions (red crosses) within the search area (large circle) are shown relative to the slip contours (green contour is used here). On the top right, the distribution of interplate aftershock distances (as measured and normalized in Fig. 5) from the slip contour (red histograms) is compared with the distribution of random positions in the search circle with corresponding distances, with the population normalized to match the number of observed events from -1.0 to 0.25. On the bottom right, the variation of area enclosed within varying rupture contours for the specific rupture model is shown.

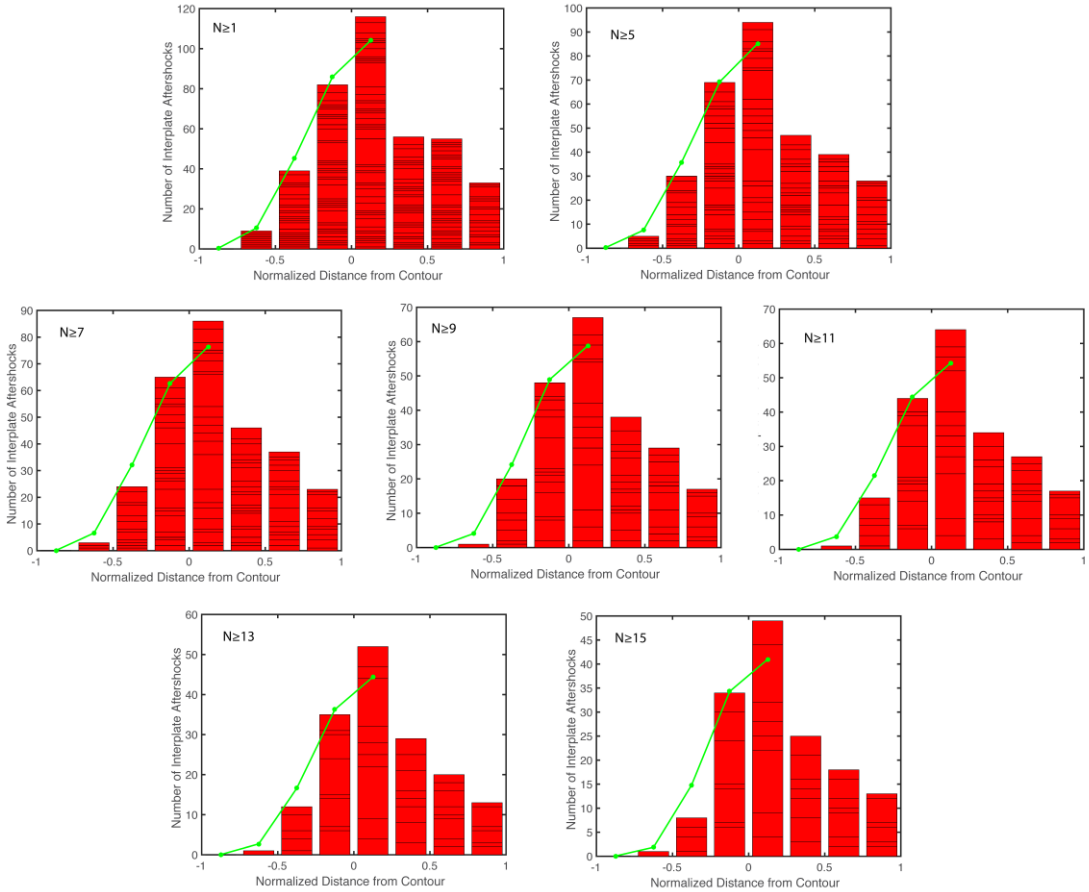

fig. S5. Cumulative distributions for varying aftershock thresholds. Stacked composite distributions of relocated aftershocks for sets of events with different number of aftershocks, N. The green curves with circles are composite reference distributions for models calculated using the specific rupture area for each event with randomly distributed seismicity with respect to the reference contour ($\Delta r = 0$) (both internally and externally). The model curves (green) are normalized so that their sum in the five intervals from -1.0 to 0.25 is equal to the sum of the observations (red bars) over these same intervals. Under this normalization a systematic deficiency in the inner bins results in an apparent surplus in aftershocks in bins -0.25 and 0.25.

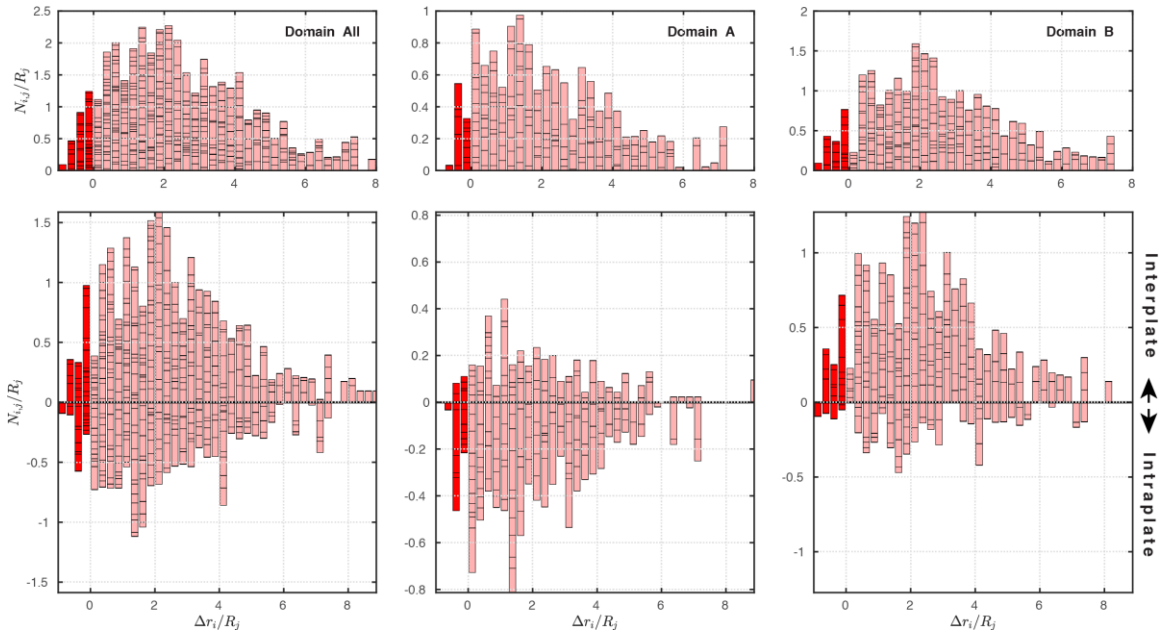

fig. S6. GCMT seismicity locations relative to mainshock slip zones. Distributions of aftershocks in the GCMT catalog with $M_W \geq 5.2$ at their minimum distance from $\chi = 0.5$ contour for A: all mainshocks), B: ruptures of at least Domain A, and C: ruptures of Domain B and deeper, with normalizations by R_j as in Fig. 3. The lower panels (D, E and F) show the corresponding subset distribution of interplate aftershocks by the positive bars, and the intraplate aftershocks by the negative bars.

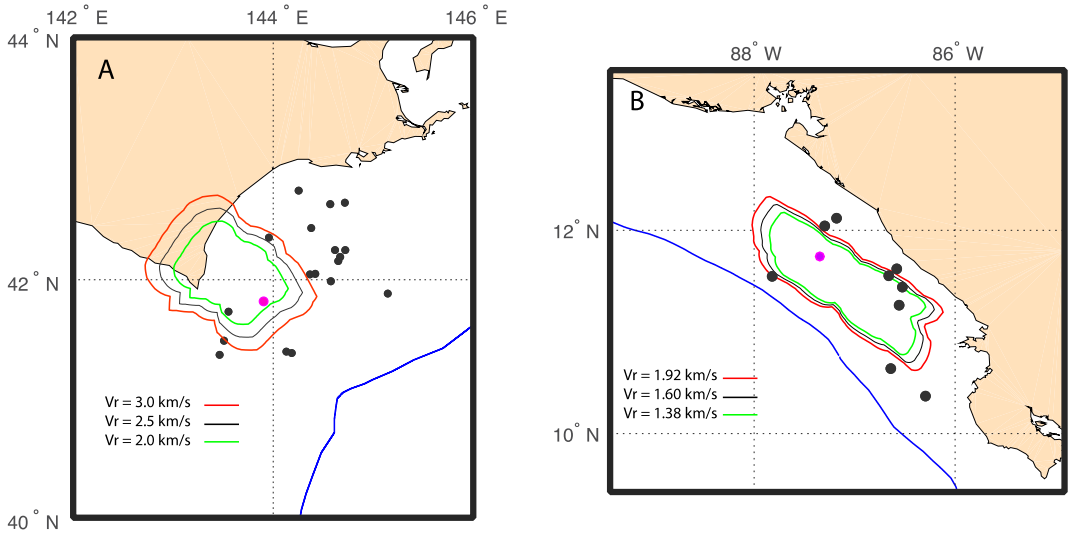

fig. S7. Examples of rupture dimension modification with ±20% change in modeled rupture velocity. The rupture contours of the χ = 0.15 portion of the peak slip for (**A**): the 25 September 2003 M_W 8.2 Hokkaido and (**B**): the 2 September 1992 M_W 7.6 Nicaragua megathrust earthquakes are shown by the black lines for the preferred rupture velocities. The variable rupture areas for 20% increased rupture velocities are shown by red lines, and for 20% reduced rupture velocities by green lines The relocated aftershocks of the GCMT catalog with $M_W \geq 5.2$ are shown by the black dots, and mainshock epicenter locations (NEIC) are shown by magenta circles.

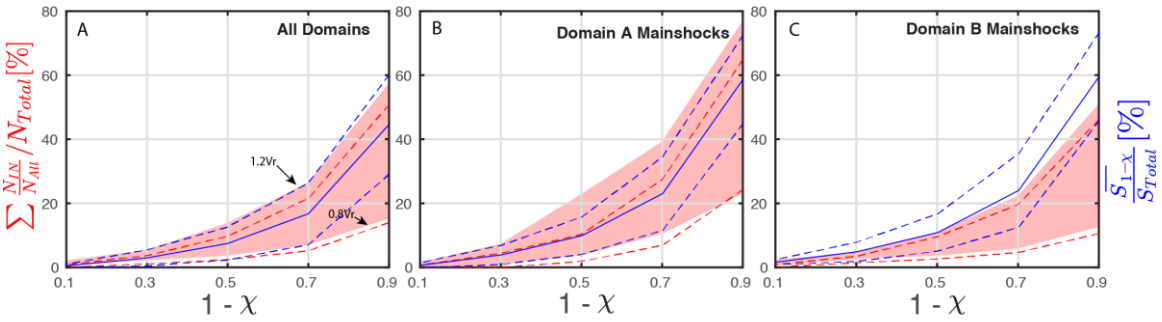

fig. S8. Seismicity locations within the mainshock slip zone. The mean ratio for all mainshocks for number of 14-day aftershocks enclosed by a mainshock slip fraction, χ, contour divided by total number of events for (**A**): all events, (**B**): shallow ruptures of at least Domain A, and (**C**): deep ruptures of Domain B or deeper. Curves are shown for the full range of source dimensions spanned by varying the rupture velocity by ±20% relative to their original estimation, resulting in about ±40% change in the rupture area. The salmon areas indicate the range of ratios for all aftershocks and the red dashed lines indicate the results for just interplate events. The blue curves indicate the cumulative fractional area for each slip fraction. Note this plot displays the overall distribution of data allowing for the uncertain source dimensions; for evaluating deficiency of activity within the slip zone the individual event behavior needs to be considered as in Fig. 5.

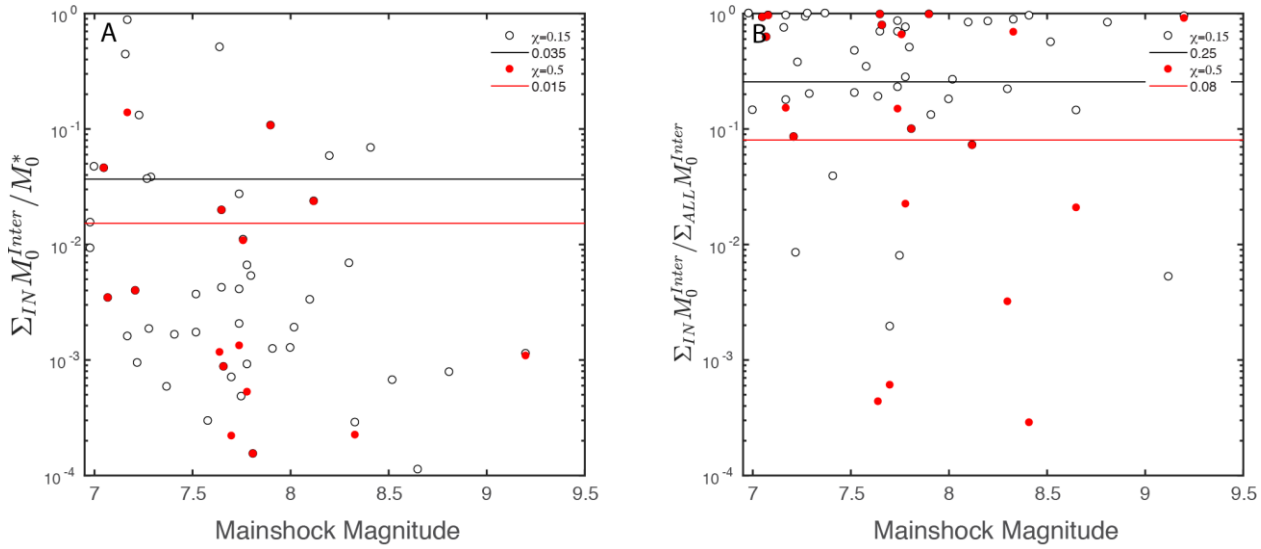

fig. S9. Cumulative seismic moment distributions. (**A**): ratios of cumulative seismic moment of interplate aftershocks enclosed by the χ = 0.15 slip contour (open circles) and the χ = 0.5 contour (red circles), divided by the mainshock seismic moment. (**B**): ratios of cumulative seismic moment of interplate aftershocks enclosed by the χ = 0.15 slip contour (open circles) and the χ = 0.5 contour (red circles), divided by the summed seismic moment of the total aftershock sequence. 37 of the 101 mainshocks have at least one aftershock within the χ = 0.15 contour; 20 have at least one aftershock within the χ = 0.5 contour. The horizontal lines present the mean values (indicated in the legend) of the two populations of each panel. The plots include all aftershocks in the GCMT catalog with $M_W \geq 5.2$. Mainshocks with no aftershocks within the contour are omitted. The measurements are shown as a function of mainshock magnitude to disaggregate the results, allowing identification of individual earthquakes. No trend with mainshock magnitude is expected or observed.